Radiotracers for Low Density Lipoprotein Biodistribution Studies In Vivo: Technetium-99m Low Density Lipoprotein Versus Radioiodinated Low Density Lipoprotein Preparations

Shankar Vallabhajosula, Michael Paidi, Juan Jose Badimon, Ngoc-Anh Le, Stanley J. Goldsmith, Valentin Fuster, and Henry N. Ginsberg

Mount Sinai School of Medicine, New York; and the College of Physicians and Surgeons, Columbia University, New York, New York

In an attempt to characterize the in vivo behavior of [^{99m}Tc] low density lipoprotein (LDL), biodistribution studies were performed in normal and hypercholesterolemic (HC) rabbits. In normal rabbits, 24 hr after the injection of [^{99m}Tc]LDL, ^{99m}Tc activity accumulated mainly in adrenal glands, spleen, liver, and kidney. In HC rabbits, however, there was a marked reduction of ^{99m}Tc activity in these organs. In both normal and HC rabbits, <17% of ^{99m}Tc activity appeared in the 24-hr urine following injection of [^{99m}Tc]LDL, suggesting that in vivo, [^{99m}Tc]LDL is trapped and accumulated within the tissues. Direct comparison of [^{99m}Tc]LDL, ^{125}I-native-LDL and [^{131}I]tyramine cellobiose-LDL (the previously validated trapped radioligand) in normal rabbits, demonstrated that the biodistribution of [^{99m}Tc]LDL was similar to that of [^{131}I]tyramine cellobiose-LDL. The adrenal glands, liver, and spleen accumulated significantly greater quantities of ^{99m}Tc and ^{131}I activity per gram of tissue than ^{125}I (from native-LDL). In addition, imaging studies in monkeys, showed that the hepatic uptake and retention of [^{99m}Tc] LDL was similar to that of [^{131}I]tyramine cellobiose LDL. In contrast, radioiodine from native-LDL was deiodinated in liver with subsequent excretion into the intestine. These results suggest that [^{99m}Tc]LDL acts as a trapped ligand in vivo and should therefore, be a good tracer for noninvasive quantitative biodistribution studies of LDL.

J Nucl Med 29: 1237–1245, 1988

The metabolism of lipoproteins has been studied in depth both in vitro and in vivo. The in vivo studies have focused upon the plasma kinetics of the metabolism of apolipoprotein-B (apo B), the major structural protein of very low-density lipoprotein (VLDL), intermediate density lipoprotein (IDL), and low density lipoprotein (LDL). Although these studies have added greatly to our understanding of the plasma lipid and lipoprotein levels in normal and diseased states, we have not, until recently been able to study the biodistribution of lipoproteins in the intact organism. The recent development of intracellularly trapped ligands such as carbon-14 (^{14}C) sucrose-LDL (*1*), and radioiodinated tyramine cellobiose-LDL (*2–4*) has permitted investigators to identify the sites of in vivo degradation of LDL in animals. These methods, however, require killing the animals, thus excluding repeat studies in the same animal or humans. In addition, neither iodine-125 (^{125}I) nor iodine-131 (^{131}I) are ideal for noninvasive imaging studies.

Noninvasive studies of lipoprotein biodistribution and of the interaction of lipoproteins with vessel wall lesions in animals and humans require a radiolabeled, trapped ligand suitable for imaging. Lees et al. (*5*) first reported the technique of labeling LDL with technetium-99m (^{99m}Tc), a radionuclide ideal for imaging studies, and obtained images of the injured, healing, arterial wall and the adrenal cortex in normal rabbits.

Received July 20, 1987; revision accepted Feb. 8, 1988.

For reprints contact: Shankar Vallabhajosula, PhD, Andre Meyer Department of Physics-Nuclear Medicine, Mount Sinai School of Medicine, One Gustave L. Levy Place, New York, New York.

After validating the purity and biologic activity of [^{99m}Tc]LDL, Lees et al. (*5*) reported that the biodistribution of human [^{99m}Tc]LDL in rabbits was similar to that of [^{125}I]LDL. However, no data directly comparing these two tracers was presented in their paper.

In contrast, our initial imaging studies in monkeys (*6*), comparing the distribution of [^{99m}Tc]LDL to that of ^{131}I-native LDL, showed that the initial ^{131}I activity in the liver gradually decreased due to deiodination, while ^{99m}Tc activity progressively accumulated within the liver. These results suggested that [^{99m}Tc]LDL was acting as a trapped ligand in vivo. To evaluate this hypothesis, we performed biodistribution studies in rabbits comparing directly the tissue accumulation of [^{99m}Tc]LDL to that of [^{131}I]tyramine cellobiose-LDL (an intracellularly trapped ligand) and ^{125}I-native-LDL. Technetium-99m LDL distribution in normal and HC rabbits was studied in order to assess the role of LDL receptors (*7,8*) on the tissue uptake of LDL.

MATERIALS AND METHODS

Separation of LDL from Plasma

LDL (d = 1.019 – 1.063 g/ml) from normal human or rabbit plasma was isolated by sequential ultracentrifugation (*9*). This procedure results in an LDL preparation in which apo-B comprises ~95% of the protein content. The apo-E content of a typical human LDL preparation is <1% as measured by RIA technique. The LDL fraction was dialyzed overnight against normal saline, pH 7.2, containing 0.1 mg/ml EDTA. The purity of LDL was studied by agarose gel electrophoresis using standard lipoprotein staining techniques. The LDL concentration was determined using the method of Lowry et al. (*10*).

Radioiodinated LDL

LDL was labeled with ^{125}I or ^{131}I using the iodine monochloride method (*11*) and the free radioiodide was removed by repetitive dialysis against 0.9% NaCl containing 0.1 mg/ml EDTA, pH 7.2. The specific activity of radioiodinated LDL preparations ranged from 50–100 μCi/mg protein. In vitro and in vivo studies in our laboratory have demonstrated that radioiodinated LDL retains full biologic and immunologic activity when stored at 4°C for 2–3 wk.

Iodine-131 tyramine cellobiose-LDL was prepared according to the method of Pittman et al. (*2*). Purified tyramine cellobiose and cyanuric acid were kindly supplied by Dr. R. Pittman. The unreacted [^{131}I]tyramine cellobiose was removed by dialysis (*2*). The [^{131}I]tyramine cellobiose-LDL was used within 48 hr of preparation. The specific activity ranged from 20–50 μCi/mg. All radioiodinated LDL preparations were used within 2 wk from the time of preparation.

Preparation of [^{99m}Tc]LDL

LDL was labeled with ^{99m}Tc by the reductive coupling of [^{99m}Tc]pertechnetate to native-LDL using sodium dithionite as a reduction agent (*5*). One to two milligrams of LDL (2–4 mg/ml) were mixed with 10–50 mCi of [^{99m}Tc]pertechnetate (0.5 ml) and 0.1 ml of glycine buffer, pH 10, containing 10 mg of sodium dithionite. The mixture was incubated for 30 min at room temperature and was then applied on a Sephadex G-25 gel column to separate [^{99m}Tc]LDL from free ^{99m}Tc. At the same time, 2 mg of human serum albumin (HSA) was also applied to the column to avoid nonspecific binding of LDL to the Sephadex gel. The column was eluted with saline and the labeling efficiency was calculated by comparing the amount of ^{99m}Tc activity eluted with LDL in the void volume to the total ^{99m}Tc activity applied to the column (incubation mixture). The stability of the gel purified [^{99m}Tc]LDL was studied by performing electrophoresis at different times over the next 24 hr. The electrophoresis was performed for 45 min on agarose plates at 2 mA constant current in pH 8.6 barbital buffer. The fraction of ^{99m}Tc bound to LDL as a function of time was estimated by measuring both the amount of ^{99m}Tc associated with LDL band and the free ^{99m}Tc. For biodistribution studies, [^{99m}Tc]LDL (3 mCi/0.1 mg), along with 0.2 mg of cold HSA was injected into the animals within 30 min of gel purification.

Biodistribution of [^{99m}Tc]LDL in Normal and HC Rabbits

Technetium-99m LDL (3 mCi/0.1 mg), from a normal rabbit was injected intravenously through an ear vein of normal rabbits (n = 4) and rabbits fed a high cholesterol (0.5%) diet for 2–3 mo (n = 5). The plasma LDL levels in these HC rabbits were four to five times above normal values (*12*). Starting from 5 min postinjection, blood samples were obtained over the next 24 hr. The distribution of [^{99m}Tc]LDL was also studied by imaging the rabbits at various times post injection using a gamma camera fitted with a high resolution, low-energy collimator. Five- to ten-minute images of at least 500,000 counts were obtained and stored in an imaging computer (Microdelta). The animals were killed at 24 hr and various organs removed and weighed. The radioactivity in the tissue samples and in an aliquot of the injection mixture was determined in a gamma counter. The amount of ^{99m}Tc activity in the organs was expressed as percent injected dose/g of the tissue. In order to calculate the total activity in muscle, small intestine and large bowel, organ weights reported by Jelenko et al. (*13*) were used. The amount of radioactivity/ml blood at different sampling times after injection of LDL into rabbits was expressed as a fraction of the total radioactivity/ml blood obtained at 5 min. These data were fitted to the sum of two exponentials using a nonlinear regression routine (*14*). The fractional catabolic rate, defined as the fraction of the plasma pool which is metabolized per unit time, was calculated from the area under the decay curve (*15*).

In order to determine the urinary excretion of free [^{99m}Tc] following the injection of [^{99m}Tc]LDL, both normal and HC rabbits were kept in metabolic cages and urine was collected for 24 hr. The amount of ^{99m}Tc activity in 24-hr total urine sample was expressed as the percent of injected [^{99m}Tc]LDL activity. In a control experiment, similar studies were performed with another group of normal rabbits (n = 4) in order to determine the amount of ^{99m}Tc activity excreted during a 24-hr period following an injection of [^{99m}Tc]pertechnetate alone.

Comparison of [^{99m}Tc]LDL, [^{125}I]LDL and [^{131}I]Tyramine Cellobiose-LDL Preparations

Biodistribution in normal rabbits. Rabbit LDL labeled with ^{99m}Tc (3 mCi/0.1 mg), ^{125}I (50 μCi/0.5 mg) and [^{131}I]tyramine cellobiose (50 μCi/1.0 mg) were injected simultaneously into

the ear vein of normal, New Zealand white rabbits (n = 4). Starting from 5 min postinjection, blood samples were obtained over the next 24 hr. The animals were killed at 24 hr and various organs removed and weighed. The ^{99m}Tc, ^{125}I, and ^{131}I activities in the tissue and blood samples were determined in a gamma counter. The ^{99m}Tc and ^{125}I counts were corrected for the cross over of ^{131}I counts. For the three radiolabeled LDL preparations, the percent injected dose/g of tissue and the fractional catabolic rates were calculated as described above.

Imaging studies in monkey. Human LDL labeled with ^{99m}Tc (3 mCi) and ^{131}I (0.1 mCi) were simultaneously administered into the antecubital vein of cynomolgus monkeys (n = 2). Thirty minutes postinjection, static images in an anterior view were obtained using a gamma camera (Picker Dyna camera 4/15) fitted with a high-energy collimator. In ^{99m}Tc window, 500,000 counts were obtained within 2–4 min of acquisition time. Due to low dose of [^{131}I]LDL injected, ~ 100,000 counts were obtained in ^{131}I window within 20 min of acquisition time. Repeat images and ten blood samples were obtained over the next 8 hrs. The images were acquired into 128 × 128 matrix using an MDS computer. Based on the time-activity curves of blood samples, the half-times of plasma clearance of [^{99m}Tc]LDL and [^{131}I]LDL were calculated.

RESULTS

Stability of [^{99m}Tc]LDL

Separation of [^{99m}Tc]LDL from free ^{99m}Tc using gel chromatography is shown in Figure 1. Technetium-99m LDL (identified by uv and radioactivity) coeluted with the cold HSA (identified by uv) in the void volume. Free ^{99m}Tc (identified by radioactivity) eluted in the salt volume. In Figure 1, the uv absorbance showing the first protein peak in the void volume represents both LDL and HSA. The second protein peak (identified by uv only) in the salt volume is due to a low molecular weight contaminant of HSA solution. Technetium-99m did not bind to HSA or to its low molecular weight contaminant. Labeling efficiency of LDL with ^{99m}Tc ranged from 30–50%. Technetium-99m LDL eluting in the void volume along with cold HSA was injected into animals for biodistribution studies.

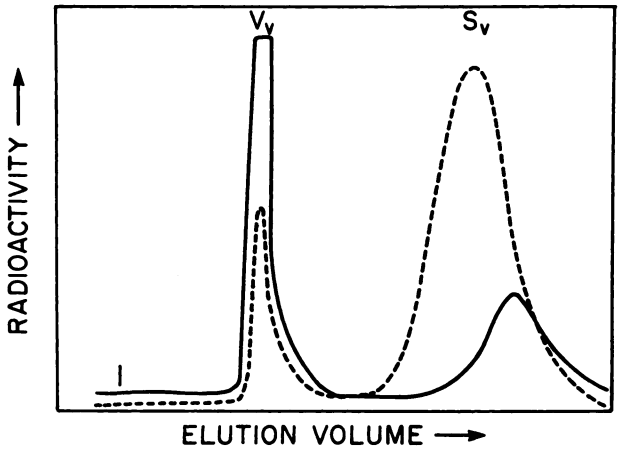

FIGURE 1
Sephadex G-25 gel chromatography of [^{99m}Tc]LDL. An incubatin mixture containing LDL, [^{99m}Tc]pertechnetate and dithionate was applied on the column along with HSA solution. [^{99m}Tc]LDL eluted in the void volume (Vv). Free (unbound) ^{99m}Tc eluted in the salt volume (Sv). The solid line depicts uv absorbance at 280 nm and the dotted line represents radioactivity.

We performed electrophoresis experiments (Fig. 2) to establish the purity of gel filtered [^{99m}Tc]LDL preparation. Figure 2C shows the electrophoretogram of an incubation mixture before purification, demonstrating the presence of two radioactive bands corresponding to [^{99m}Tc]LDL and free ^{99m}Tc. Figure 2D shows an electrophoretogram of gel purified [^{99m}Tc]LDL showing only one radioactive band without any contamination of free ^{99m}Tc. Only the slower radioactive peaks in Figures 2C and 2D stained for the lipoprotein, similar to the unlabeled LDL (Fig. 2A), thus establishing the purity and integrity of [^{99m}Tc]LDL. The percent of total ^{99m}Tc activity associated with LDL on the agarose plate was calculated at different times after gel purification by performing repeat electrophoresis of aliquots of a

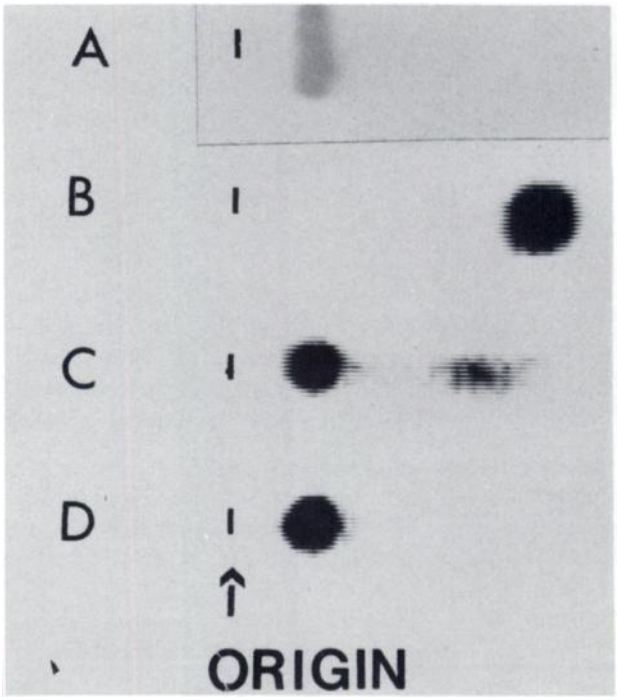

FIGURE 2
Electrophoresis of gel filtered [^{99m}Tc]LDL: Comparison with unlabeled LDL and free ^{99m}Tc. Native LDL was stained with Fat Red 7B lipid stain and ^{99m}Tc activity was detected using gamma camera imaging. A: Native LDL showing a single band close to the origin. B: Free [^{99m}Tc]pertechnetate (a single band) migrates significantly faster than LDL. C: An incubation mixture of LDL, [^{99m}Tc]pertechnetate, and dithionite showing two bands of radioactivity representing [^{99m}Tc]LDL and free ^{99m}Tc. D: Gel filtered [^{99m}Tc] LDL showing a single radioactive band corresponding to the migration of native-LDL (A).

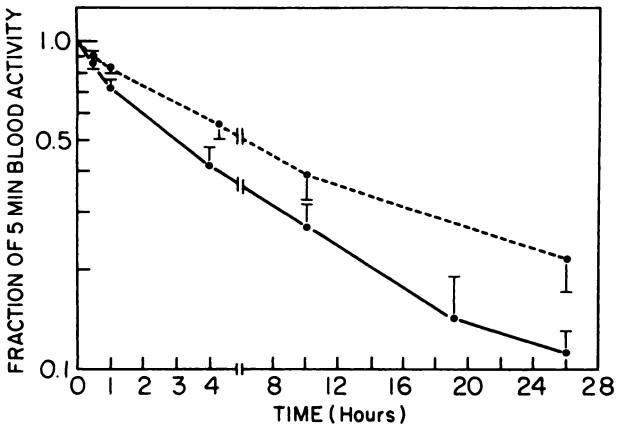

FIGURE 3
Plasma decay curves of [^{99m}Tc]LDL in normal and hypercholesterolemic (HC) rabbits. The disappearance of [^{99m}Tc]LDL was slower in HC rabbits (dotted line) compared to normal rabbits (solid line).

preparation stored at room temperature. Fifteen minutes after separation of [^{99m}Tc]LDL from the Sephadex column, 95% of the ^{99m}Tc activity was bound to the LDL. During the next 6 hr about 10% of the ^{99m}Tc activity dissociated from the LDL. After 24 hr storage, 75% of the ^{99m}Tc activity was still associated with the LDL band. For in vivo studies, [^{99m}Tc]LDL was injected into rabbits, within 30 min after gel purification.

Biodistribution of [^{99m}Tc]LDL in Rabbits

The disappearance of rabbit [^{99m}Tc]LDL from the circulation in normal control rabbits and HC rabbits is shown in Figure 3. The fractional catabolic rate of [^{99m}Tc]LDL in HC rabbits (1.05 ± 0.43 day^{-1}) was lower than that in normal rabbits (2.97 ± 1.8 day^{-1}).

The biodistribution of [^{99m}Tc]LDL in normal and HC rabbits is compared in Table 1. In both groups, total accumulation of ^{99m}Tc by the liver predominated. When the results were expressed as percent injected dose/g of tissue, the 24 hr uptake of ^{99m}Tc in normal rabbits was highest in the adrenal glands (1.34 ± 0.58), followed by spleen (0.84 ± 0.26), liver (0.46 ± 0.10) and kidney (0.18 ± 0.05). In HC rabbits, however, the uptake of ^{99m}Tc in the adrenal glands (0.12 ± 0.04), spleen (0.23 ± 0.11), and liver (0.23 ± 0.04) was significantly reduced. In HC rabbits, the kidney uptake (0.29 ± 0.13) was increased. Even when the slower clearance of [^{99m}Tc]LDL from plasma of HC rabbits was taken into account, the 24-hr uptake by the adrenals was markedly reduced compared to normal rabbits.

The urinary excretion of ^{99m}Tc radioactivity within a 24-hr period following an injection of [^{99m}Tc]LDL was 16 ± 3% in normal rabbits and 17 ± 4% in HC rabbits. In contrast, most of the ^{99m}Tc radioactivity (71 ± 11) was excreted in the urine within a 24-hr period following an injection of [^{99m}Tc]pertechnetate alone.

The gamma camera images of [^{99m}Tc]LDL distribution in normal and HC rabbits, obtained 24 hr postinjection are shown in Figure 4. In normal rabbits, the uptake of ^{99m}Tc activity in adrenals, spleen liver, and kidney is clearly visualized. In HC rabbits, however, the adrenal glands were not seen and there was a marked reduction of ^{99m}Tc uptake in liver and spleen. In addition, the uptake of ^{99m}Tc activity by the kidneys in HC rabbits was greater than in normal rabbits. Also an increased uptake of ^{99m}Tc activity above the liver (corresponding to the area of aorta) was clearly seen in the HC rabbit. The distribution of [^{99m}Tc]LDL in normal and HC rabbits seen by the gamma camera images (Fig. 4) was similar to the biodistribution results (Table 1) obtained after sacrificing the animals and counting the radioactivity in tissues.

Comparison of [^{99m}Tc]LDL, [^{125}I]LDL and [^{131}I]Tyramine Cellobiose-LDL Preparations

Biodistribution studies in rabbits. The disappearance of three radiolabeled rabbit LDL preparations (^{99m}Tc,

TABLE 1
Technetium-99m LDL Distribution in Normal and Hypercholesterolemic (HC) Rabbits

	Percent of injected dose at 24 hr in			
	Normal rabbits (n = 4)		HC rabbits (n = 5)	
Organ	Per gram	Per organ	Per gram	Per organ
Blood	0.03 ± 0.01	5.10 ± 1.60	0.09 ± 0.03	19.80 ± 6.60
Adrenals	1.34 ± 0.58	0.31 ± 0.13	0.12 ± 0.04	0.08 ± 0.03
Spleen	0.84 ± 0.26	1.46 ± 0.45	0.23 ± 0.11	0.97 ± 0.46
Liver	0.46 ± 0.10	35.70 ± 7.75	0.23 ± 0.04	28.37 ± 4.90
Kidney	0.18 ± 0.05	3.00 ± 0.83	0.29 ± 0.13	6.26 ± 2.80
Bone marrow	0.11 ± 0.05	6.80 ± 3.10	0.12 ± 0.04	9.60 ± 3.20
Gall bladder	0.10 ± 0.03	0.11 ± 0.03	0.09 ± 0.08	0.23 ± 0.20
Lungs	0.04 ± 0.03	0.46 ± 0.34	0.05 ± 0.01	0.72 ± 0.15
Aorta	0.03 ± 0.01	—	0.09 ± 0.01	—
Small bowel	0.016 ± 0.001	1.47 ± 0.10	0.018 ± 0.005	2.15 ± 0.60
Large bowel	0.014 ± 0.001	1.22 ± 0.10	0.018 ± 0.005	2.02 ± 0.60
Gonads	0.005 ± 0.001	0.04 ± 0.01	0.008 ± 0.004	0.09 ± 0.05
Muscle	0.005 ± 0.002	8.45 ± 3.34	0.007 ±0.003	15.40 ± 6.60

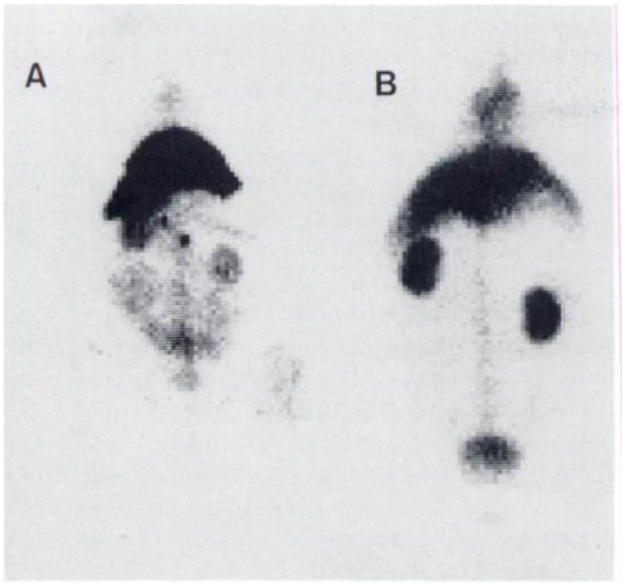

FIGURE 4
Gamma camera images of ^{99m}Tc activity in normal (A) and HC (B) rabbits were obtained 24 hr after the injection of [^{99m}Tc]LDL. The images show intense uptake by liver, adrenals, and spleen in normal rabbits and reduced uptake by liver and spleen with non-visualization of adrenals in HC rabbits. The kidney uptake in HC rabbits is much greater than in normal rabbits.

^{125}I, and [^{131}I]tyramine cellobiose) from the circulation in normal rabbits is shown in Figure 5. The fractional catabolic rate of [^{99m}Tc]LDL (2.97 ± 1.78 day^{-1}) was similar to that of ^{125}I-native-LDL (3.07 ± 2.23 day^{-1}) suggesting that these two tracers were behaving similarly in the circulation. Iodine-131 tyramine cellobiose-LDL had a slower fractional catabolic rate (1.0 ± 0.15 day^{-1}) suggesting that its rate of plasma clearance was lower than that of either ^{125}I- or ^{99m}Tc-labeled LDL.

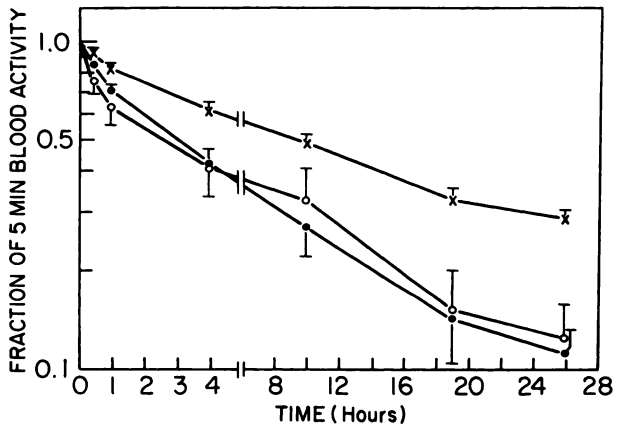

FIGURE 5
Plasma decay curves of [^{99m}Tc]LDL, [^{125}I]LDL, and [^{131}I] tyramine cellobiose-LDL. The plasma disappearance of [^{99m}Tc]LDL (●) and [^{125}I]LDL (○) were quite similar and more rapid than the disappearance of [^{131}I]tyramine cellobiose-LDL (X).

The accumulation of the three radiolabeled LDL preparations in several selected tissues is summarized in Table 2. Although the amount of radioactivity remaining in blood (0.05%) was similar at 24 hr for both [^{99m}Tc]LDL and ^{125}I-native-LDL, there was a significant difference in the tissue distribution of radioactivity. The accumulation of ^{99m}Tc was ten times higher in adrenals (2.02 ± 1.03), spleen (0.74 ± 0.59) and liver (0.46 ± 0.08) compared to the uptake of ^{125}I in these three tissues (0.23 ± 0.23, 0.08 ± 0.03, 0.06 ± 0.02, respectively). The uptake of ^{131}I (from tyramine cellobiose-LDL) in adrenals (1.23 ± 0.56), spleen (0.62 ± 0.20) and liver (0.22 ± 0.03) was some what less than that of ^{99m}Tc, but also significantly higher than the uptake of ^{125}I (from native-LDL). Since the blood activity of [^{131}I] tyramine cellobiose-LDL (0.15 ± 0.02%) was three times higher than [^{99m}Tc]LDL at 24 hr, direct comparison of the tissue uptake of these two tracers is difficult. These results do indicate, however, that [^{99m}Tc]LDL behaved much more like the trapped ligand, [^{131}I]tyramine cellobiose-LDL than like ^{125}I-native-LDL.

Imaging studies in monkeys. The simultaneous plasma disappearance curves of human [^{99m}Tc]LDL and [^{131}I]LDL from the circulation of a monkey are depicted in Figure 6. The amounts of radioactivity remaining at various times postinjection were expressed as a fraction of radioactivity in the first sample obtained at 15 min. The half-times of plasma clearance (4.5 hr) of ^{99m}Tc- and ^{131}I-labeled LDL were identical, suggesting that in the circulation [^{99m}Tc]LDL was behaving in a manner similar to [^{131}I]LDL. When the biodistribution of these two tracers was studied by gamma camera imaging at different times postinjection (Fig. 7), however, significant differences were observed. Within one hour, both tracers had similar distributions as 40% of the injected activity of each tracer was in the liver. Due to intense uptake of radioactivity in the liver, the relatively small amounts of radioactivity in other organs

TABLE 2
Comparison of the Accumulation of Three LDL Radiotracers in Selected Tissues of Normal Rabbits

	Percent injected dose per gram of tissue at 24 hr		
Organ	[^{99m}Tc]LDL	[^{131}I]tyramine cellobiose-LDL	^{125}I-native-LDL
Blood	0.05 ± 0.03*	0.15 ± 0.02	0.05 ± 0.05
Adrenals	2.02 ± 1.03	1.23 ± 0.56	0.23 ± 0.23
Spleen	0.74 ± 0.59	0.62 ± 0.20	0.08 ± 0.03
Liver	0.46 ± 0.08	0.22 ± 0.03	0.06 ± 0.02
Kidney	0.17 ± 0.05	0.28 ± 0.09	0.03 ± 0.02
Gall bladder	0.13 ± 0.10	0.10 ± 0.08	0.07 ± 0.04
Lungs	0.07 ± 0.04	0.07 ± 0.03	0.05 ± 0.03

* Mean ± s.d. (n = 4).

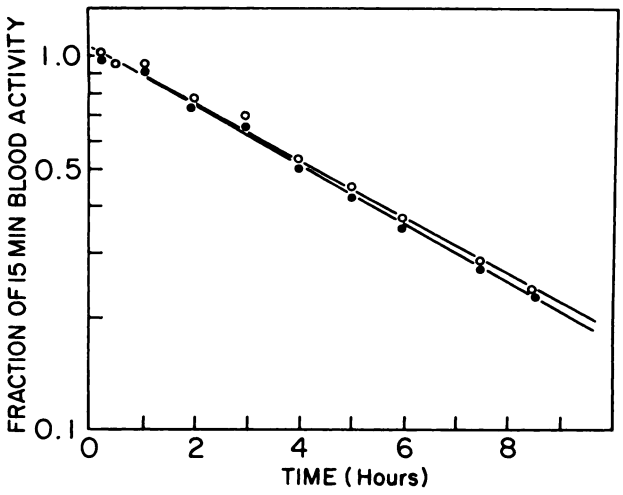

FIGURE 6
Plasma decay curves of [^{99m}Tc]LDL (●) and [^{131}I]LDL (○) in a monkey. The disappearance of both tracers from the circulation was identical.

was not visible. Over the next 8 hr, however, ^{131}I activity in the liver diminished significantly while ^{99m}Tc activity taken up by the liver remained within that organ. During this time period, ^{131}I activity accumulated in the area of lower abdomen below the liver. In contrast, when similar imaging studies were performed after injecting human [^{99m}Tc]LDL and [^{131}I]tyramine cellobiose-LDL into a normal monkey, both tracers behaved similarly. The liver was the major organ accumulating each tracer and neither the ^{131}I nor the ^{99m}Tc activities in the liver diminished during the 8 hr of this study (Fig. 8). These results also suggest that [^{99m}Tc]LDL, like [^{131}I]tyramine cellobiose-LDL, remained trapped within the liver.

DISCUSSION

Tissue distribution of radiolabeled LDL will depend upon the stability and biologic integrity of the tracer. Lees et al. (*5*) have already shown that [^{99m}Tc]LDL was stable to electrophoresis, ultrafiltration and passage in vivo. In addition, they also reported that immunoelectrophoresis of [^{99m}Tc]LDL produced a single precipitin arc against anti-LDL antiserum similar to native-LDL. In our studies we confirmed the purity and in vitro stability of [^{99m}TC]LDL by electrophoresis (Fig. 2). After gel purification, 95% of the ^{99m}Tc activity was bound to the LDL. When stored at room temperature for 6 hr, 90% of the ^{99m}Tc activity was still bound to the LDL. In all our studies, [^{99m}Tc]LDL was injected into the animals within 30 min of gel purification.

In normal control rabbits, the disappearance of [^{99m}Tc]LDL from circulation reflects a biexponential decay mode (Fig. 3). The fractional catabolic rates of [^{99m}Tc]LDL and ^{125}I-native-LDL (Fig. 5) were similar, suggesting that in circulation [^{99m}Tc]LDL behaves similar to radioiodinated native-LDL. These FCR values are in agreement with those of several other studies in the literature in which only radioiodinated native-LDL was used (*16–18*). A review of rabbit LDL kinetic papers reveals a wide range of FCRs but several studies have rates that are essentially the same as ours. Lees et al. (*5*) reported a half-time of about 20 hr for human [^{99m}Tc]LDL injected into rabbits, based on only the major, slower component of the die-away curve. The percent injected dose remaining in circulation at 24 hr postinjection in our studies (Table 1) was essentially the same as the value reported by Lees et al. (*5*).

In normal rabbits, 24 hr after the injection of [^{99m}Tc]LDL, 35% of ^{99m}Tc activity accumulated within the liver. Adrenal glands, however, accumulated a greater percentage of ^{99m}Tc activity per gram of tissue, followed by spleen, liver, and kidney. The order of [^{99m}Tc]LDL uptake in these organs was similar to the observations of Lees et al. (*5*), although the absolute amounts varied. In their biodistribution studies in rabbits, Lees et al. (*5*) used human LDL, whereas we used normal rabbit LDL. This may partially account for the differences in FCRs and absolute tissue distribution data between our results and their results. The pattern of biodistribution of [^{99m}Tc]LDL in our studies is similar to those observed with [^{14}C]sucrose-LDL (*1*) and [^{125}I]tyramine cellobiose-LDL (*2,3*) preparations.

The FCR of [^{99m}Tc]LDL in HC rabbits, was lower than that in normal rabbits (Fig. 3). At 24 hr 20% of the injected dose still remained in circulation compared to only 5% in normal rabbits (Table 1). In addition, there were significant reductions in the uptake of ^{99m}Tc activity in all the major organs except kidneys. Some of the reduced uptake by tissues in HC rabbits may be due to increased plasma pool of LDL. But the significant reduction observed in the uptake by the adrenal glands, may indicate the role of LDL receptors in the uptake process. The accumulation of ^{99m}Tc by the adrenals in HC rabbits was only 10% of the accumulation observed in normal rabbits. Adrenal glands have the highest LDL receptor activity per gram of tissue (*3*) and are expected to be most affected by dietary induced hypercholesterolemia with subsequent down-regulation of LDL receptors (*8,19*).

Intracellular trapping of [^{99m}Tc]LDL should be associated with minimal urinary excretion of ^{99m}Tc activity. In both normal and HC rabbits (Table 1), ~17% of ^{99m}Tc activity was excreted in urine collected over the 24-hr period following an injection of [^{99m}Tc]LDL. In a control experiment, 70% of ^{99m}Tc activity appeared in the urine within a 24-hr period following an injection of [^{99m}Tc]pertechnetate alone. In addition, in unpublished human studies (n = 9) with [^{99m}Tc]LDL, we have observed that only 5–12% of ^{99m}Tc activity was excreted in the urine during the first 24 hr after injection.

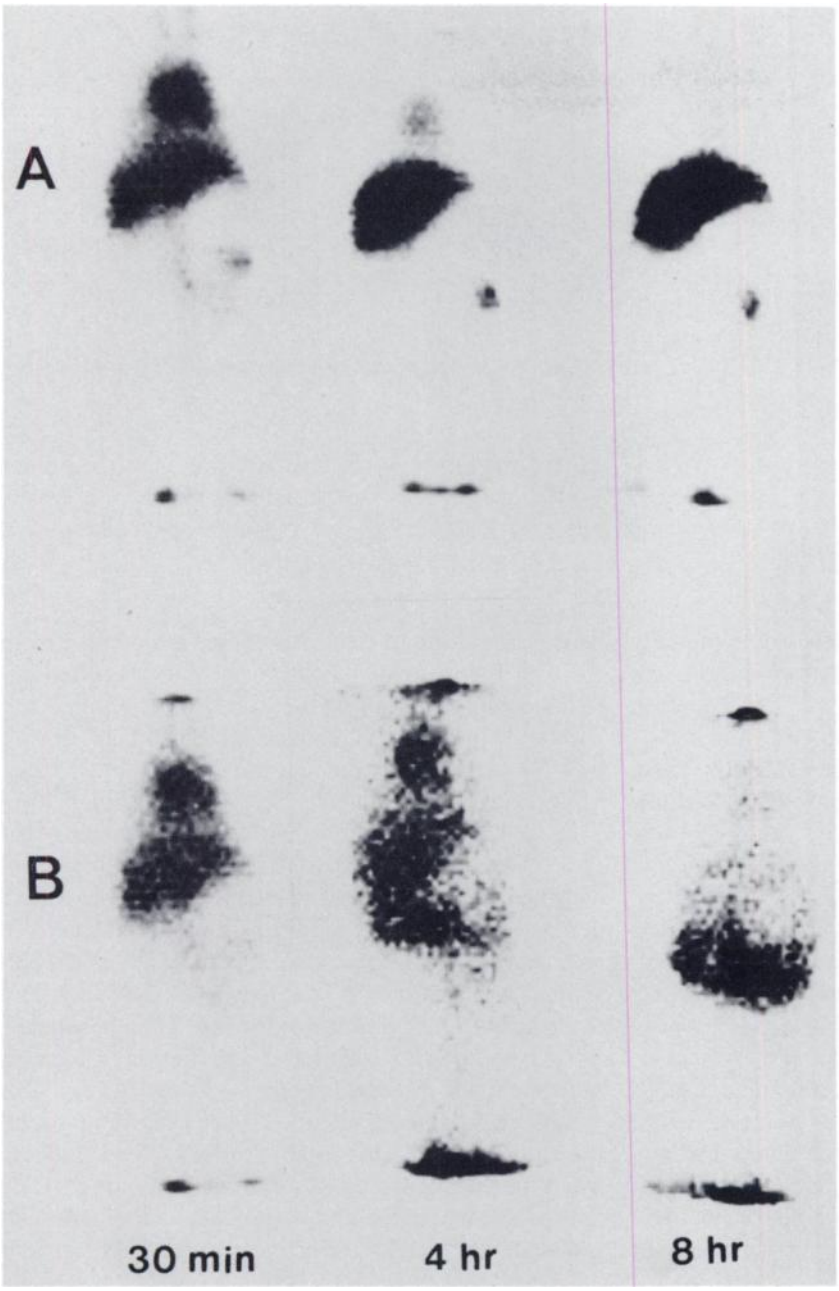

FIGURE 7
Gamma camera images of [^{99m}Tc] LDL and [^{131}I]LDL distribution in a normal monkey. Technetium-99m (A) and ^{131}I (B) activities rapidly accumulated in liver. Over the next 8 hr, while ^{99m}Tc activity was retained in the liver, the ^{131}I activity, however, was rapidly and progressively released into lower abdomen.

In normal rabbits, the plasma decay curves of [^{99m}Tc] LDL and ^{125}I-native-LDL were identical (Fig. 5) suggesting that the stability and behavior of [^{99m}Tc]LDL in circulation was similar to that of radioiodinated-native-LDL. At 24 hr, however, there was significantly less ^{125}I activity accumulated in most of the tissues measured (Table 2). In organs with the most active uptake, ^{125}I activity was only 10–20% of what was observed with ^{99m}Tc activity, indicating that the deiodination occurred uniformly throughout the body. These results clearly show that greater amounts of [^{99m}Tc]LDL accumulated within the tissues and was retained compared to radioiodinated native-LDL.

The plasma decay of [^{131}I]tyramine cellobiose LDL was slower than that of [^{99m}Tc]LDL (Fig. 5). Since the plasma decay of [^{99m}Tc]LDL was identical to that of ^{125}I-native-LDL, we believe that our [^{131}I]tyramine cellobiose-LDL tracer was removed in an abnormally slow manner. This belief is supported by similar, although less dramatic differences in the disappearance of ^{131}I-native-LDL and [^{131}I]tyramine cellobiose-LDL in monkeys reported by Portman et al. (*3*). In addition, slower removal of tyramine cellobiose-LDL has been observed in some, but not all preparations synthesized by Pittman and his co-workers (Pittman R: personal communication).

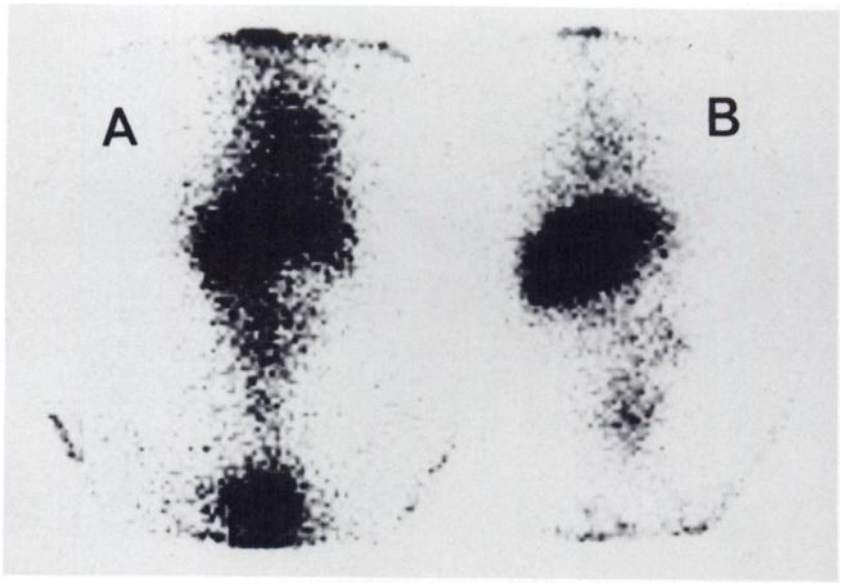

FIGURE 8
Gamma camera images of [^{131}I]tyramine cellobiose-LDL distribution in a monkey. After the injection, the tracer accumulated in liver with in 30 min (A) and was retained there over the next 8 hr (B).

In contrast to the difference between radioiodinated native-LDL and [^{99m}Tc]LDL that we observed, the tissue distribution studies comparing [^{99m}Tc]LDL and [^{131}I]tyramine cellobiose-LDL revealed that these two ligands behaved quite similarly (Table 2). Both ^{99m}Tc and ^{131}I were taken up and retained by the various tissues and organs. The pattern of distribution of each radiotracer per gram of tissue was similar, although the accumulation of ^{131}I activity in adrenals, spleen and liver was less than the accumulation of ^{99m}Tc activity in these organs. These differences probably resulted from both the slower removal of the [^{131}I]tyramine cellobiose-LDL from plasma noted above and the leakage of [^{131}I]tyramine cellobiose from tissues. Pittman et al. (*2*) observed that the tyramine cellobiose ligand appears to leak from catabolizing cells at a rate of ~10% a day. In addition, they observed a high rate of leakage from rabbit liver. Despite these differences between these two traces, the results strongly support our conclusion that the [^{99m}Tc]LDL acts as a biologically active trapped ligand.

Noninvasive imaging of LDL distribution in vivo would avoid the need to kill the animals for tissue uptake measurements. The imaging studies of [^{99m}Tc]LDL in normal and HC rabbits (Fig. 4) clearly show the differences in tissue distribution that were observed by actually counting tissue samples (Table 1). Similarly, the differences observed in the biodistribution studies in rabbits between the [^{99m}Tc]LDL and the ^{131}I-native-LDL were clearly seen in the imaging studies performed in monkeys. The early images revealed equivalent accumulation of radioactivity over the liver (Fig. 7). Over the next several hours, however, the ^{131}I radioactivity diminished dramatically from the area of the liver and was seen best over the lower abdominal area, probably within the lumen of intestine. This late appearance of ^{131}I activity over the area of the intestine (Fig. 7) is, we believe, the result of clearance of free radioiodine from the liver following deiodination of LDL. Technetium-99m activity taken up by the liver, however, remained within the liver (Fig. 7), with no subsequent appearance of ^{99m}Tc activity over the lower abdomen.

In contrast, the imaging studies comparing [^{99m}Tc]LDL and [^{131}I]tyramine cellobiose-LDL revealed that these two tracers behave quite similarly. The images of a normal monkey (Fig. 8) injected with these two tracers demonstrated that the accumulation and retention of radioactivity within liver over a period of 8 hours was similar, and that the ^{99m}Tc activity was trapped within the liver like [^{131}I]tyramine cellobiose. These results are in agreement with the tissue distribution studies in normal rabbits discussed above.

Although radioiodinated LDL has been quite useful for studying the plasma catabolism of LDL in vivo, the use of this tracer for biodistribution studies is severely limited by the rapid and significant deiodination of radioiodinated LDL within the tissues. This problem has been evident in both imaging (*20,21*) and tissue distribution studies. The availability of a biologically trapped lipoprotein radiotracer that can be imaged by standard nuclear imaging cameras will provide investigators new tools for studying lipoprotein metabolism in vivo. This tracer would facilitate studies of the effects of diet and drugs upon LDL receptor activity, of the biodistribution of LDL in various hyperlipidemias as well as hypolipidemias (*22,23*), and of the sites of catabolism of lipoproteins other than LDL (*20,24*).

REFERENCES

1. Pittman RC, Attie AD, Carew TE, Steinberg D. Tissue sites of degradation of low density lipoprotein: application of method for determining the fate of plasma proteins. *Proc Natl Acad Sci USA* 1979; 76:5345–5349.

2. Pittman RC, Carew TE, Glass CK, Green SR, Taylor CA, Attie AD. A radioiodinated, intracellularly trapped ligand for determining the sites of plasma protein degradation *in vivo*. *Biochem J* 1983; 212:791–800.
3. Pittman RC, Carew TE, Attie AD, Witztum JL, Watanabe Y, Steinberg D. Receptor-Dependent and receptor-independent degradation of low density lipoprotein in normal rabbits and in receptor-deficient mutant rabbits. *J Biol Chem* 1982; 257:7994–8000.
4. Portman OW, Alexander M. Metabolism of ^{125}I-tyramine cellobiose-labeled low density lipoproteins in squirrel monkeys. *Atherosclerosis* 1985; 56:283–289.
5. Lees RS, Garabedian HD, Lees AM, et al. Technetium-99m low density lipoproteins: preparation and biodistribution. *J Nucl Med* 1985; 26:1056–1062.
6. Vallabhajosula S, Ginsberg HN, Badimon JJ, et al. Evaluation of ^{99m}Tc-LDL for studying lipoprotein metabolism and imaging atherosclerotic lesions *in vivo* [Abstract]. *J Nucl Med* 1985; 26:P131.
7. Goldstein JL, Brown MS. The low-density lipoprotein pathway and its relation to atherosclerosis. *Ann Rev Biochem* 1977; 46:897–930.
8. Kovanen PT, Brown MS, Basu SK, Bilheimer DW, Goldstein JL. Saturation and suppression of hepatic lipoprotein receptors: a mechanism for the hypercholesterolemia for cholesterol-fed rabbits. *Proc Natl Acad Sci USA* 1981; 78:1396–1400.
9. Havel RJ, Eder HA, Bragdon JH. The distribution and chemical composition of ultracentrifugally separated lipoproteins in human serum. *J Clin Invest* 1955; 34:1345–1353.
10. Lowry OH, Rosebrough NJ, Farr AL, Randall RJ. Protein measurement with the Folin phenol reagent. *J Biol Chem* 1951; 193:265–275.
11. McFarlane AS. Efficient trace-labelling of proteins with iodine. *Nature* 1958; 182:53.
12. Badimon JJ, Kottke B, Chen TC, Chen L, Mao SJT. Quantification and immuno localization of apolipoprotein E in experimental atherosclerosis. *Atherosclerosis* 1986; 61:57–66.
13. Jelenko C, Anderson AP, Scott TH, Wheeler ML. Organ weights and water composition of the New Zealand albino rabbit. *Am J Vet Rest* 1971; 32:1637–1639.
14. Berman M, Weiss M. SAAM Manual, Department of HEW, Washington DC, Publication No (NIH)78-180, 1978.
15. Matthews CME. The theory of tracer experiments with ^{131}I-labeled plasma proteins. *Phys Med Biol* 1957; 2:36–53.
16. Peluffo RO, Nervi AM, Gonzalez S, Brenner RR. Turnover of low density lipoproteins in normal and atherosclerotic rabbits. *Acta Physiol Latinoam* 1983; 33:33–44.
17. Stoudemire JB, Renaud G, Shames DM, Havel RJ. Impaired receptor-mediated catabolism of low density lipoproteins in fasted rabbits. *J Lipid Res* 1984; 25:33–39.
18. Carew TE, Pittman RC, Marchand ER, Steinberg D. Measurement *in vivo* of irreversible degradation of low density lipoprotein in the rabbit aorta. *Arteriosclerosis* 1984; 4:214–224.
19. Brown MS, Goldstein JL. Lipoprotein receptors in the liver. Control signals for plasma cholesterol traffic. *J Clin Invest* 1983; 72:743–747.
20. Roberts AB, Lees AM, Lees RS, et al: Selective accumulation of low density lipoprotein in damaged arterial wall. *J Lip Res* 1983; 24:1160–1167.
21. Huetting M, Corbett JR, Schneider WJ, Willerson JT, Brown MS, Goldstein JL. Imaging of hepatic low density lipoprotein receptors by radionuclide scintiscanning *in vivo*. *Proc Natl Acad Sci USA* 1984; 81:7599–7603.
22. Ginsberg H, Goldberg IJ, Wang-Iverson P, et al. Increased catabolism of native and cyclohexandeione-modified low density lipoprotein in subjects with myeloproliferative diseases. *Arteriosclerosis* 1983; 3:233–241.
23. Ginsberg H, Grabowski GA, Gibson JC, et al. Reduced plasma concentrations of total, low density lipoprotein and high density lipoprotein cholesterol in patients with Gaucher Type 1 disease. *Clin Gen* 1984; 26:109–116.
24. Funke H, Boyles J, Weisgraber KH, Ludwig EH, Hui DY, Mahley RW. Uptake of apolipoprotein E-containing high density lipoproteins by hepatic parenchymal cells. *Arteriosclerosis* 1984; 4:452–461.